

## SiGe-Mixing-Triggered Rapid-Melting-Growth of High-Mobility Ge-on-Insulator

Taizoh Sadoh<sup>a</sup>, Kaoru Toko, Masashi Kurosawa, Takanori Tanaka, Takashi Sakane, Yasuharu Ohta, Naoyuki Kawabata, Hiroyuki Yokoyama, and Masanobu Miyao<sup>b</sup>

Department of Electronics, Kyushu University, 744 Motooka, Fukuoka, 819-0395, Japan

<sup>a</sup>sadoh@ed.kyushu-u.ac.jp, <sup>b</sup>miyao@ed.kyushu-u.ac.jp

**Keywords:** Ge on insulator, Liquid phase epitaxy, Large scale integrated circuit

**Abstract.** We have investigated the Si-seeding rapid-melting process and demonstrated the formation of giant Ge stripes with (100), (110), and (111) orientations on Si (100), (110), and (111) substrates, respectively, covered with SiO<sub>2</sub> films. We revealed that crystallization is triggered by Si-Ge mixing in the seeding regions in this process. Based on this mechanism, we have proposed a novel technique to realize orientation-controlled Ge layers on transparent insulating substrates by using Si artificial micro-seeds with (100) and (111)-orientations. This achieved epitaxial growth of single crystalline (100) and (111)-oriented Ge stripes on quartz substrates. The Ge layers showed a high hole mobility exceeding 1100 cm<sup>2</sup>/Vs owing to the high crystallinity.

### Introduction

Research and development of new functional devices that enable ultrahigh speed operation, ultralow power dissipation, and multi-functional operation are required in order to break through the scaling limit of the transistor performance. In line with this, group IV-based heterostructure technologies have been widely developed over the last quarter century [1]. The high quality Ge layers on insulators (GOI) are promising materials for this purpose. High-speed Ge-channel thin film transistors (TFTs) are essential devices to realize system-in-displays and three-dimensional (3D) large scale integrated circuits (LSIs). Moreover, GOI structures are also important as channel materials of spintransistors and virtual substrates of direct-band gap materials with optical functions to create multifunctional 3D-LSIs [2].

In line with this, we have been developing SiGe mixing triggered liquid-phase epitaxy (LPE) [3]. This achieves high-mobility Ge single crystals on transparent insulating substrates [4]. The present paper reviews our recent progress in this novel growth technique [3-7].

### Experimental Procedure

Si(100), (110), and (111) wafers covered with SiO<sub>2</sub> films (50 nm thickness) were used as substrates. The SiO<sub>2</sub> films were patterned by wet etching to form seeding window areas, where SiO<sub>2</sub> layers were locally removed. Subsequently, amorphous-Ge (a-Ge) layers (100 nm thickness) were deposited using a solid-source molecular beam epitaxy (MBE) system (base pressure: 5×10<sup>-11</sup> Torr), and they

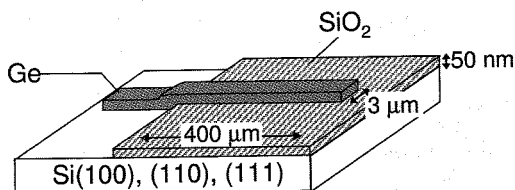


Figure 1. Schematic sample structure.

were patterned into narrow stripes (400  $\mu\text{m}$  length, 3  $\mu\text{m}$  width), as shown in Fig. 1. Then  $\text{SiO}_2$  capping-layers were deposited by RF magnetron sputtering. Finally, these samples were heat-treated by rapid thermal annealing (RTA) at 1000°C (1 sec), to induce liquid-phase epitaxial growth from the seeding areas.

## Results and Discussion

**SiGe Mixing-Triggered-Growth from Si Substrates.** The electron backscattering diffraction (EBSD) images of the samples grown on Si (100), (110), and (111) substrates are shown in Figs. 2(a), 2(b), and 2(c), respectively. These results indicate that the single crystalline Ge layers with the crystal orientations identical to those of Si substrates are grown on  $\text{SiO}_2$  layers for all samples. This clearly means that crystal growth is initiated at the Si seeding areas and propagates laterally over  $\text{SiO}_2$  films. It is found that the lateral growth length exceeds several hundreds  $\mu\text{m}$ , which is one order longer than those reported in the previous works [8]. The cross-sectional transmission electron microscopy (TEM) observation of the sample revealed very high defect density at the Si/Ge interface regions in the seeding areas due to the lattice mismatch ( $\sim 4\%$ ) between Si and Ge, but no dislocation or stacking fault in the laterally-grown regions. These defect-necking results well agree with those for the previously reported experiments [8]. In this way, giant lateral growth over several hundreds  $\mu\text{m}$  is demonstrated.

The crystal quality was evaluated by micro-probe Raman spectroscopy (spot size:  $\sim 1 \mu\text{m}\phi$ ) as a function of the distance from the seeding area. The full-width at half maximum (FWHM) of the main Raman peaks ( $296.8 \text{ cm}^{-1}$ ) originating from the vibration mode for Ge-Ge of the (100) sample shown in Fig. 2(a) is summarized in Fig. 3(a), where FWHM obtained from a single crystalline Ge wafer is also shown for comparison. The FWHM values in the seeding area are about  $4\text{--}5 \text{ cm}^{-1}$ , which is wider than that of single crystalline Ge ( $3.2 \text{ cm}^{-1}$ ). However, almost equal values ( $\sim 3.3 \text{ cm}^{-1}$ ) to single-crystalline Ge are obtained from the laterally-grown area, indicating the high crystal quality. The FWHM values obtained from the laterally-grown areas of the samples shown in Figs. 2(b) and 2(c) were also as small as  $\sim 3.3 \text{ cm}^{-1}$ .

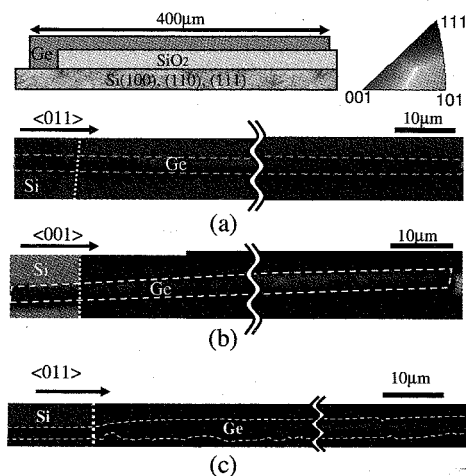


Figure 2. (Color online) EBSD images for samples grown with Si(100) (a), (110) (b), and (111) seeding substrates (c).

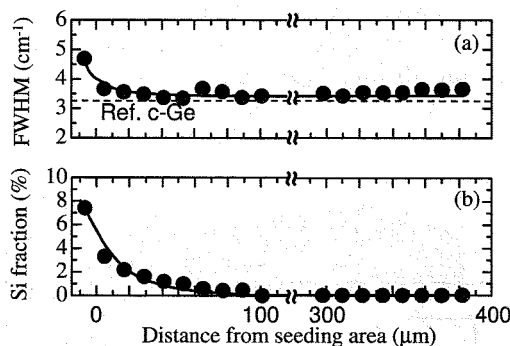


Figure 3. FWHM of Raman peak due to Ge-Ge bonds (a) and Si fraction distribution in Ge layers (b) for the sample grown with Si (100) seeding substrate.

To examine the Si diffusion in laterally-grown regions, the Si fraction was evaluated from the Raman peaks ( $380.9\text{ cm}^{-1}$ ) originating from the vibration mode for Si-Ge, as a function of the distance from the seeding area. The result is summarized in Fig. 3(b). It is found that the Si fraction in the seeding area and the seeding edge are 8 and 4%, respectively. It gradually decreases along the growth direction and reaches to zero at a distance exceeding  $70\text{ }\mu\text{m}$ . Consequently, pure single crystalline Ge is obtained in the large region between  $70$  and  $400\text{ }\mu\text{m}$  from the seeding edge.

In order to explain this rapid-melting process, there are two possible important driving forces initiating the lateral growth of Ge on  $\text{SiO}_2$  layers. A thermal flow from the liquid SiGe or Ge region to the Si substrate through seeding window is an important factor to be considered as a trigger for the lateral growth as revealed by Tamura et al. in the seeding lateral liquid-phase epitaxial growth of Si using the Q-switched pulse ruby laser irradiation [9]. Another important factor is the spatial gradient of the Si fraction existing in and near the seeding area (distance  $< 50\text{ }\mu\text{m}$ ), as shown in Fig. 3(b). Since the solidification temperature of  $\text{Si}_x\text{Ge}_{1-x}$  ( $0 < x < 1$ ) increases with increasing Si fraction ( $x$ ), i.e.,  $939^\circ\text{C}$  for Ge and  $1412^\circ\text{C}$  for Si, melt-back should be initiated at the Si-rich region in the seeding area. Solidification starts just after RTA ( $1000^\circ\text{C}$ ), however, SiGe at the seeding edge (Si fraction: 4%, solidification temperature:  $970^\circ\text{C}$ ) is still melting. Thus, relatively large difference in the solidification temperature is generated. Consequently, melt-back propagates along this large gradient of the solidification temperature.

In order to separate the effects of such different two factors, an additional experiment was carried out [3]. In this experiment, quartz substrates ( $600\text{ }\mu\text{m}$  thickness) were employed in order to suppress thermal flow from the liquid Ge regions to the substrates through seeding windows. In the experiment, poly-Si ( $100\text{ nm}$  thickness) was deposited on quartz substrates and patterned by wet etching to form seeding areas. Subsequently, a-Ge layers ( $100\text{ nm}$  thickness) were deposited and patterned into narrow stripe lines ( $3\text{ }\mu\text{m}$  width,  $400\text{ }\mu\text{m}$  length).

It is worth noting that the EBSD observations of the samples after RTA indicated that single crystal growth was initiated from the poly-Si seed and propagated laterally over  $400\text{ }\mu\text{m}$  length. On the other hand, poly-Ge layers were obtained, when poly-Ge was employed as the seeds instead of poly-Si. These results clearly indicate that solidification temperature gradient by Si-Ge mixing is the dominant factor triggering the lateral growth, as schematically shown in Fig. 4(a). To reveal the orientation control phenomenon of Ge stripes, we performed a statistical analysis of crystal orientations of grains in poly-Si seeds and those of Ge layers near the poly-Si seeds. The orientation distributions of Ge layers near the Si-seeds quite agreed with those of poly-Si seeds. This indicates that one of the crystal-grains in the poly-Si island incidentally acts as the seed to cause the rapid-melting growth of the Ge stripes.

To explain the giant lateral growth of pure Ge obtained in the region far from the seeding area, another driving force should be considered. This is because the gradient of the Si fraction does not exist in this region, as shown in Fig. 3(b). The latent heat of solidification at the solid-liquid interface is a key factor to explain this phenomenon. In the cooling process after RTA, the temperature of the

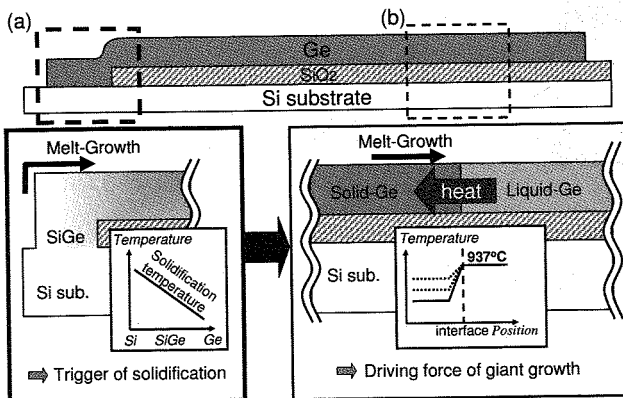


Figure 4. Growth mechanism of GOI near (a) and far beyond seeding area (b).

solid-Ge falls with time. However, the molten-Si tends to keep a constant melting-temperature due to latent heat. Consequently, a thermal gradient is automatically formed at the growth front, which realizes the continuous lateral growth for such a long distance as schematically shown in Fig. 4(b).

**High Quality GOI with Si Artificial Micro-Seed.** These findings triggered an idea of the directional lateral growth of a-Ge on transparent insulators using Si artificial micro-crystals instead of Si-substrates to obtain orientation-controlled GOI structures by a Si-substrate free process. Orientation control of the Si micro-crystal seeds is essential for this process. We have already established a technique to form Si crystal grains oriented to (100) or (111) by the interfacial-oxide-modulated Al-induced crystallization (AIC) [5], as shown in Figs. 5(a)-5(c). This interfacial-oxide modulated AIC technique enables the creation of the Si artificial micro-seeds orientated to (100) and (111).

By using the Si artificial micro-seeds, we examined epitaxial growth of single crystalline Ge stripes on quartz substrates. The EBSD measurements revealed that giant ( $> 100 \mu\text{m}$  length) single crystal GOI with (100) and (111) orientations were obtained by using the (100) and (111)-oriented Si micro-seeds, respectively. Crystal structures of the grown layers are characterized by TEM. The results of (100)-oriented GOI are shown in Fig. 6. The results indicate no dislocation or stacking fault in the grown layer. In this way, formation of high quality single-crystalline Ge (100) and (111) stripes becomes possible even on transparent insulating substrates by using the Si artificial micro-seeds.

The electrical characteristics of Ge stripes are also evaluated for many samples by measuring the temperature dependence of the electrical conductivity. This demonstrated the high hole mobility of  $1150 \pm 50 \text{ cm}^2/\text{Vs}$  for all samples. Very sharp dispersion of the mobility distribution ( $1150 \pm 50 \text{ cm}^2/\text{Vs}$ ) indicates that the orientation-controlled rapid melting growth enables the uniform-formation of single-crystalline Ge stripe arrays on insulating substrates. The hole mobility and hole concentration of the GOI structures obtained by the present method are summarized in Fig. 7, together with those by the conventional GOI structures obtained by solid-phase crystallization (SPC) [10] and oxidation-induced Ge-condensation techniques [11]. The GOI structures obtained by the present method show electrical characteristics superior to those by the conventional methods, due to the high crystallinity. Consequently, orientation-controlled GOI structures with high hole mobility exceeding  $1100 \text{ cm}^2/\text{Vs}$  have been realized by the Si-substrate-free process.

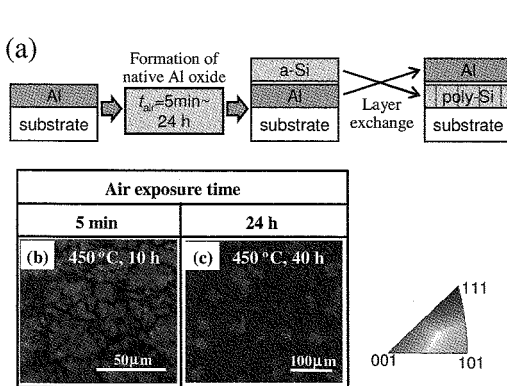


Figure 5. (Color online) Process flow of AIC (a) and EBSD images of poly-Si layers grown by AIC (air exposure time: 5 min (b) and 24 h (c)).

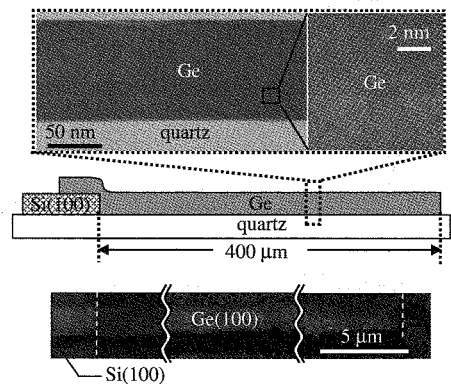


Figure 6. (Color online) EBSD and cross-sectional TEM images of the (100)-oriented GOI layer.

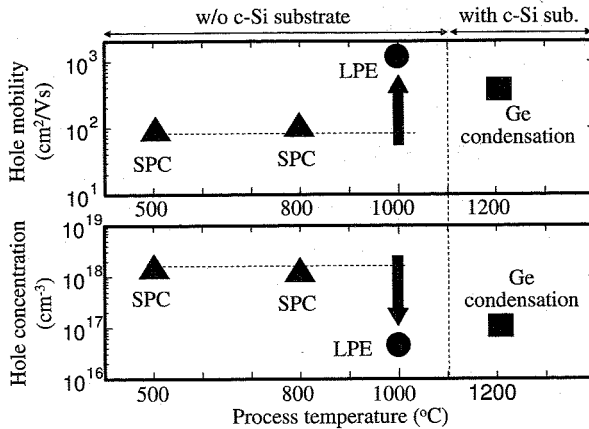


Figure 7. Comparison of hole mobility and concentration in GOI grown by present method (LPE), together with those obtained by SPC [10] and Ge-condensation [11].

## Summary

The SiGe mixing-triggered rapid-melting-growth of GOI has been investigated. It has been demonstrated that the driving force to trigger the lateral growth of Ge is the spatial gradient of the solidification temperature originating from Si-Ge mixing at seeding areas. Based on this mechanism, a novel technique to obtain orientation-controlled Ge layers on transparent substrates by using the Si artificial micro-seeds has been proposed. The interfacial-oxide modulated AIC method enables the (100) or (111)-oriented micro-seed. Consequently, giant lateral growth ( $>100\ \mu\text{m}$ ) of Ge (100) and (111) layers with high crystallinity and hole mobility ( $>1100\ \text{cm}^2/\text{Vs}$ ) has been realized on transparent substrates. This SiGe mixing-triggered growth technique opens up the possibility of high-performance TFTs and virtual substrates for multifunctional 3D-LSIs.

## Acknowledgements

The authors wish to thank Dr. I. Mizushima, Dr. N. Tamura, and Dr. M. Yoshimaru of Semiconductor Technology Academic Research Center (STARC) for valuable discussion and comments. A part of this work was supported by STARC and a Grant-in-Aid for Scientific Research from the Ministry of Education, Culture, Sports, Science, and Technology in Japan.

## References

- [1] M. Miyao and K. Nakagawa: Jpn. J. Appl. Phys. Vol. 33 (1994), p. 3791
- [2] Y. Ando, K. Hamaya, K. Kasahara, Y. Kishi, K. Ueda, K. Sawano, T. Sadoh, and M. Miyao: Appl. Phys. Lett. Vol. 94 (2009), p. 1832105, K. Hamaya, K. Ueda, Y. Kishi, Y. Ando, T. Sadoh, and M. Miyao: Appl. Phys. Lett. Vol. 93 (2008), p. 132117, K. Hamaya, H. Itoh, O. Nakatsuka, K. Ueda, K. Yamamoto, M. Itakura, T. Taniyama, T. Ono, and M. Miyao: Phys. Rev. Lett. Vol. 102 (2009), p. 137204
- [3] M. Miyao, T. Tanaka, K. Toko, and M. Tanaka: Appl. Phys. Express Vol. 2 (2009), p. 045503
- [4] M. Miyao, K. Toko, T. Tanaka, and T. Sadoh: Appl. Phys. Lett. Vol. 95 (2009), p. 022115
- [5] M. Kurosawa, N. Kawabata, T. Sadoh, and M. Miyao: Appl. Phys. Lett. Vol. 95 (2009), p. 132103
- [6] K. Toko, T. Sakane, T. Tanaka, T. Sadoh, and M. Miyao: Appl. Phys. Lett. Vol. 95 (2009), p. 112107

- 
- [7] T. Tanaka, K. Toko, T. Sadoh, and M. Miyao: Appl. Phys. Express, Vol. 3 (2010), p. 031301
- [8] Y. Liu, M. D. Deal, and D. Plummer: Appl. Phys. Lett. Vol. 84 (2004), p. 2563, D. J. Tweet, J. J. Lee, J. S. Maa, and S. T. Hsu: Appl. Phys. Lett. Vol. 87 (2005), p. 141908, F. Gao, S. J. Lee, S. Balakumar, A. Du, Y-L. Foo, and D-L. Kwong: Thin Solid Films Vol. 504 (2006), p. 69, S. Balakumar, M. M. Roy, B. Ramamurthy, C. H. Tung, G. Fei, S. Tripathy, C. Dongzhi, R. Kumar, N. Balasubramanian, and D. L. Kwog: Electrochemical and Solid-State Lett. Vol. 9 (2006), p. G158, T. Hashimoto, C. Yoshimoto, T. Hosoi, T. Shimura, and H. Watanabe: Appl. Phys. Express Vol. 2 (2009), p. 066502
- [9] M. Tamura, H. Tamura, M. Miyao, and T. Tokuyama: Jpn. J. Appl. Phys. Vol. 20, Suppl.20-1 (1981), p. 43
- [10] K. Toko, I. Nakao, T. Sadoh, T. Noguchi, and M. Miyao: Solid-State Electron. Vol. 53 (2009), p. 1159
- [11] T. Maeda, K. Ikeda, S. Nakaharai, T. Tezuka, N. Sugiyama, Y. Moriyama, and S. Tkagi: Thin Solid Films Vol. 508 (2006), p. 346